ELSEVIER

Biochimica et Biophysica Acta 1327 (1997) 131–147

BIOCHIMICA ET BIOPHYSICA ACTA
BBA

Phosphatidylcholine–fatty acid membranes: effects of headgroup hydration on the phase behaviour and structural parameters of the gel and inverse hexagonal (H_{II}) phases

John M. Seddon [a,*], Richard H. Templer [a], Neil A. Warrender [a], Zhi Huang [a], Gregor Cevc [b], Derek Marsh [c]

[a] *Department of Chemistry, Imperial College of Science, Technology and Medicine, Exhibition Road, South Kensington, London SW7 2AY, UK*

[b] *Medizinische Biophysik, Technischer Universität München, Klinikum r.d.I., Ismaningerstrasse 22, D-1675 München, Germany*

[c] *Max-Planck Institut für Biophysikalische Chemie, Abteilung Spektroskopie, D-37077 Göttingen, Germany*

Received 16 January 1997; accepted 24 February 1997

Abstract

The phase behaviour and structural parameters of a homologous series of saturated diacyl phosphatidylcholine/fatty acid 1:2 (mol/mol) mixtures having chain lengths from C_{12} to C_{20} were studied by X-ray diffraction and calorimetry, as a function of water content. The chain–melting transition temperatures of the 1:2 PC/FA mixtures are found to be largely independent of the degree of hydration. For all chain lengths, the tilted $L_{\beta'}$ and rippled $P_{\beta'}$ gel phases of the pure PC component are replaced by an untilted L_{β} gel phase in the 1:2 PC/FA mixtures. This gel phase swells considerably upon hydration, with a limiting water layer thickness in the range 18–24 Å, depending on the chain length. However, unlike pure phospholipid systems, the lateral chain packing within the gel phase bilayers is essentially identical in both the dry and the fully hydrated states. The fluid bilayer L_{α} phase is suppressed in the 1:2 mixtures, being replaced by inverse non-lamellar phases for all chain lengths greater than C_{12}, and at all levels of hydration. For chain lengths of C_{16} and greater, the inverse hexagonal H_{II} phase is formed directly upon chain melting, at all water contents. For the shorter chain length mixtures, the behaviour is more complex, with the H_{II} phase forming at low hydration, but with bicontinuous cubic phases appearing at higher levels of hydration. The implications of these surprising results are explored, in terms of the effective hydrophilicity of the associated PC and FA headgroups and the packing within the interfacial region. We suggest that the presence of the fatty acids significantly alters the lateral stress profile across the lipid monolayer in the fluid state, compared to that of the corresponding pure PC system, such that inverse phases, where the interface bends towards the water, become strongly

Abbreviations: PC, phosphatidylcholine; DLPC, 1,2-dilauroyl-*sn*-glycero-3-phosphocholine; DMPC, 1,2-dimyristoyl-*sn*-glycero-3-phosphocholine; DPPC, 1,2-dipalmitoyl-*sn*-glycero-3-phosphocholine; DSPC, 1,2-stearoyl-*sn*-glycero-3-phosphocholine; DAPC, 1,2-di-arachinoyl-*sn*-glycero-3-phosphocholine; FA, fatty acid; LA, lauric acid; MA, myristic acid; PA, palmitic acid; SA, stearic acid; AA, arachidic acid; T_m, chain–melting transition temperature

* Corresponding author. Fax: +44 171 594 5801. E-mail: J.SEDDON@IC.AC.UK

PII S0005-2736(97)00047-3

favoured. Furthermore, for short chain lengths, packing constraints favour the formation of phases with negative interfacial Gaussian curvature, such as the bicontinuous cubic phases, rather than the H_{II} phase, which has more severe chain packing frustration.

Keywords: Phosphatidylcholine/fatty acid membrane; Lipid/amphiphile mixture; Inverse hexagonal phase; Gel phase; Cubic phase; Lipid hydration

1. Introduction

Biomembranes generally contain mixtures of various types of amphiphilic molecules, such as phospholipids, glycolipids, fatty acids, diglycerides, and so on. Furthermore, these components vary in chain length, saturation, type of chain linkage, etc. This complexity has so far precluded the development of a satisfactory molecular theory to explain their liquid crystalline properties and, to date, most of our qualitative understanding of this aspect of membrane systems has been built up from studies of pure, synthetic lipid components. The binary phase diagrams of many membrane lipids in water are now well established. However, it is clear that lipid mixtures may exhibit entirely different phase behaviour from single component lipid systems. This is in part because of the possibility of intermolecular interactions, such as hydrogen bonding, between the lipid components, and in part because the possibility for microscopic partial segregation of the lipid components may relax certain packing constraints in the system. As a first step towards understanding more complex lipid mixtures, we have studied ternary systems consisting of phosphatidylcholine, fatty acid, and water.

Although present at levels of only a few percent, fatty acids are important constituents of biomembranes. Evidence is emerging that they can affect many physiological functions, such as enzyme activity [1], particularly the activation of lipid-metabolising enzymes, and calcium transport [2]. Arachidonic acid, released from membrane phospholipids by receptor mediated activation of phospholipases A_2 or C, is now believed to serve as an important second messenger in various cells [3]. The addition of free fatty acids to cell membranes can also modify other biological functions, such as fusion [4,5], platelet aggregation [6], calcium transport by sarcoplasmic reticulum [7] and direct regulation of ion channels [8]. In addition, there are certain diseases, such as Refsum's disease, where a build-up of fatty acids in nerve membranes causes a disintegration of the myelin sheath [9]. It has been known for some time that unsaturated fatty acids, which are fusogenic agents, can induce formation of the H_{II} phase upon addition to certain phospholipid or cell membranes [10,11]. A recent study has explored the fusion capability of PC/FA liposomes [12]. The PC/FA/water system thus forms a biologically relevant and, equally importantly, a potentially tractable model of how lipid mixtures can exhibit changes in the macroscopic phase behaviour from that of single lipid systems. The remainder of this introduction forms a brief review of previous studies of hydrated PC/FA systems.

Early studies showed that the addition of long-chain saturated fatty acids to phosphatidylcholines suppresses the pre-transition and broadens the gel–fluid transition, shifting it to higher temperatures [13–18]. At a fatty acid mole fraction of 0.67, the chain–melting transition in excess pH 7 buffer was found to be essentially as sharp as that of the pure phosphatidylcholine, indicating the formation of a 2:1 complex [14]. The chain–melting enthalpy ΔH_m per half-complex was found to be 17.5 kJ mol^{-1} and 35.2 kJ mol^{-1} for 1:2 DLPC/LA and DPPC/PA mixtures, respectively, very similar to the values observed for the corresponding fully hydrated pure phosphatidylcholines. In a study by X-ray diffraction and ^{31}P-NMR of the hydrated DPPC/PA (1:2) mixture, we found that the calorimetric transition observed at 61°C did not correspond to the expected gel–fluid bilayer (L_β–L_α) transition; instead, the fluid lamellar (L_α) phase was completely suppressed and the gel phase transformed directly into the inverse hexagonal (H_{II}) phase [19].

Pseudo-binary phase diagrams of saturated PC/FA mixtures in excess water have been presented, and show peritectic behaviour, along with a maximum azeotropic point close to a fatty acid mole fraction of

0.67 (i.e., a 1:2 stoichiometry) [20–23]. A theoretical analysis of the form of the phase diagram indicated that the azeotropic point is due to a combination of compound formation in the gel phase and nearly ideal mixing in the fluid phase [21]. At compositions close to the 1:2 stoichiometry the gel phase melts directly to the H_{II} phase [19,21,22,24]. Upon lowering the fatty acid mole fraction, an unidentified fluid phase was observed before the L_{α} phase appeared at lower fatty acid contents [22]. Similarly, a further unidentified phase was found at fatty acid compositions above 0.75, before the isotropic phase appeared. Low concentrations of fatty acids have been found to suppress the metastability of the gel phase of PC [25]. However, the L_{β} gel phase of the 1:2 PC/FA complex is itself metastable, apparently reverting upon incubation to a lamellar co-crystal [22].

The behaviour of mixtures of PC with long chain fatty alcohols or amines is very similar to that of PC/FA mixtures, with evidence for 1:2 complex formation [26]. It was argued that the phase behaviour of FA/PC mixtures is strongly influenced by hydrogen bonding between the fatty acids and the PC headgroups, even in the presence of excess water [27]. Thermolabile liposomes with a high fusion efficiency at 42°C can be made from DPPC/fatty alcohol (1:2, mol/mol) mixtures [28].

Other work has provided further indirect evidence of fatty acid–phospholipid headgroup interactions. A fluorescence polarization study of lymphocyte membranes found that saturated fatty acids tend to order the headgroup region of the bilayer, without altering the hydrocarbon chain packing [29]. The effect of *cis*-unsaturated fatty acids was different, tending also to order the headgroup region but to disorder the chain region. The differences between the two classes of fatty acids were interpreted as implying the presence of coexisting gel and fluid domains in the membrane. On the other hand, a ^{2}H-NMR study found that incorporation of 20 mol% PA in DPPC fluid bilayers had an ordering effect along the whole length of the phospholipid chains, the effect being strongest in the plateau region of the order parameter profile [30].

Spin label EPR experiments on DMPC/MA 1:2 mixtures indicated that the fatty acid chain is located approximately one methylene group deeper than the *sn*-2 chain of the DMPC in the H_{II} phase [31]. An X-ray study of gel phase multilayers of DPPC containing 40 mol% brominated PA found that the bromine at carbon C_2 of the PA is located close to the glycerol group of the DPPC [32]. Furthermore, unlike pure DPPC bilayers, the bilayer thickness did not change with the level of hydration. This latter feature was attributed to a loss of chain tilt for the hydrated samples in the presence of the fatty acid.

The behaviour of PC/FA 1:2 mixtures with chain lengths of C_{14} or less is more complex than that of the longer chain length mixtures. In a neutron scattering study of fully hydrated DMPC/MA 1:2 mixtures, we observed co-existing inverse hexagonal (H_{II}) and inverse bicontinuous cubic (Q_{II}) phases at 51°C [33]. The cubic phase was tentatively indexed as space group Im3m (Q^{229}), with a lattice parameter which decreased steeply from 205 Å at 54.5°C to 151 Å at 65.9°C. However, an X-ray diffraction study on the same system [34] identified this cubic phase as having Pn3m symmetry, although the space group Im3m could not be ruled out. Furthermore, evidence for an Fd3m cubic phase in DMPC/MA 1:2 mixtures has been presented [35]. A separate paper will describe the complex cubic phase behaviour of C_{12} and C_{14} PC/FA mixtures (R.H. Templer, J.M. Seddon, N.A. Warrender, A. Syrykh, Z. Huang, P. Duesing, R. Winter and J. Erbes, submitted for publication).

In an earlier paper [24], we examined the effects of protonation, salt concentration, temperature and chain length on the colloidal and phase properties of PC/FA membranes. In the present work, we describe the transitional properties and phase behaviour of a homologous series of 1:2 (mol/mol) PC/FA mixtures, with regard to the L_{β} gel and H_{II} phases, and we compare and contrast the structural parameters of the anhydrous and fully hydrated systems.

2. Materials and methods

2.1. Chemicals

The phospholipids used in this work were purchased from Avanti Polar Lipids Inc., Birmingham, Alabama, USA, and Fluka Chemie AG, Buchs, Switzerland. The fatty acids were obtained from Fluka, Aldrich Chemical Co., Gillingham, UK, and BDH Chemicals Ltd., UK. In every case the commer-

cial materials were of the highest purity available (> 99%). This was confirmed by thin-layer chromatography and the lipids were subsequently used without further purification. Solvents (chloroform, cyclohexane and methanol) were obtained from Aldrich. HPLC grade water, used throughout the experiments for preparing samples, was supplied by FSA Laboratory Supplies, England. Pure heavy water (deuterium oxide; 99.9 atom% D) for lipid density determination was obtained from Aldrich.

2.2. X-ray sample preparation

Unaligned X-ray samples were prepared from lyophilised lipids. Lipids were dissolved in either cylcohexane or a mixture of cyclohexane and chloroform (approximately 3:1). Sometimes a few drops of methanol were also required to dissolve the longer chain materials ($> C_{18}$). The mixture was thickened by evaporation until it had the consistency of treacle and was then frozen. Solvent sublimation was carried out with the sample under vacuum in an ice bath, when cyclohexane was used, and in slowly evaporating liquid nitrogen for the other solvent mixtures. To ensure the samples were as dry as possible they were weighed, placed in a desiccator, and then weighed periodically, using a Perkin Elmer AD2B autobalance (accuracy ± 0.01 mg), until no further mass loss was observed. The dried lipid components were then carefully weighed out to give a molar ratio of FA/PC of 2.000 ± 0.002. In these calculations it was assumed that the phosphatidylcholines were in fact the dihydrates. The mixtures were re-dissolved and pipetted into pre-weighed, thin walled (≈ 10 μm) X-ray capillary tubes (EG&G Astrophysics, Windsor, UK) before being lyophilised. Once dried, the sample was weighed and water added by micro-syringe to give the required water content (at this stage it was assumed that the two fatty acids displaced the two water molecules bound to the PC). It should be noted that, under these conditions, where the pH of the water is close to 6, but in any event has very little buffering capacity, the fatty acids remain essentially fully protonated (the fatty acid pK in 2:1 MA/DMPC mixtures has been determined to be 7.1 at low ionic strength at 25°C [24]). Protonated long chain fatty acids have a low solubility in water: based on data reported in [36], we estimate the aqueous solubilities at 25°C of C_{12}–C_{20} fatty acids (lauric to arachidic acid) to lie in the range 4 mM to 0.06 μM, with increasing chain length. A typical specimen contained approximately 5 mg of lipid in a 1.5 mm diameter tube, giving a sample depth of a few millimetres. Sample tubes were flame sealed to maintain a fixed level of hydration. For excess water samples the water content was 75 wt% or greater. Where water was added a homogeneous dispersion was ensured by gently warming the sample to 100°C and repeatedly centrifuging it up and down inside the sealed capillary tube, or by incubating the samples above their chain melting transition temperatures for up to 2 days.

2.3. X-ray measurements

Two X-ray diffraction systems were employed in making our measurements, one being based upon a line source and the other upon a high intensity point source. The former system consisted of a Philips PW1130 X-ray generator operating at 40 kV and 30 mA with a fine focus tube with a copper target. A Guinier bent quartz crystal monochromator set to isolate Cu-$K_{\alpha 1}$ radiation ($\lambda = 1.5405$ Å) was used to focus the X-ray beam. An electrically heated copper block which accommodated the X-ray capillaries was used to control sample temperature to an accuracy of ± 0.5°C in the range 25–200°C. An electronic temperature ramp allowed us to vary the temperature of the sample linearly with time, whilst the X-ray diffraction pattern was continuously recorded on a film which was scanned vertically behind a narrow (3 mm) horizontal X-ray aperture. Typically, the heating/cooling rate was 10°C h^{-1}, and the scanning rate of the film holder was 0.15 mm min^{-1}. The accuracy with which transition temperatures could be determined from the scans is estimated to be ± 2°C. The camera was operated under vacuum to reduce air scatter. Diffraction could be measured out to a reciprocal spacing ($s = 2 \sin\theta/\lambda$) of $s \approx 0.3$ Å^{-1}. The parasitic scatter in the beam limited the low angle measurements to $s \approx 0.01$ Å^{-1} or greater. The error in measurement of lattice parameters for this X-ray camera is estimated to be ± 0.5 Å or better.

The X-ray point source was provided by an Elliott GX20 rotating anode X-ray generator. We used a micro-focus source to give us a 100×100 μm^2 spot

at a beam current of 25 mA, and a 30 kV accelerating potential. The copper K_β and continuum background were initially filtered with respect to the K_α lines using a 20 μm thick Ni filter. Diffraction patterns were obtained using a purpose-built Franks double-mirror small-angle scattering camera. It was possible to make measurements covering the range $0.002\ \text{Å}^{-1} \leq s \leq 0.3\ \text{Å}^{-1}$ using this system. The samples were held vertically in a close-fitting, cylindrical copper jacket, whose temperature was controlled to within ± 0.03°C in the range -30 to $+100$°C, using two thermoelectric devices under computer control. The diffraction was recorded on a quantum limited, opto-electronic area detector [37]. The detector, temperature controller and X-ray shutter were controlled by a microcomputer, using a program called TV4, developed by Professors S.M. Gruner and E.F. Eikenberry, Princeton University, and subsequently revised by us to accommodate differences in hardware. We estimate that the lattice parameter measurements made with this system had a precision of ± 0.2 Å or better. The great benefit of using the optoelectronic detector was in its ability to detect single X-rays. This meant that, for the low scattering power samples investigated here, diffraction patterns were observable in a matter of a few tens of seconds, and photometrically accurate images took a few tens of minutes to record.

2.4. Differential scanning calorimetry

Measurements were made using a Perkin-Elmer DSC-2C calorimeter, interfaced to a personal computer. Samples (5–10 mg of lipid mixture) were weighed into hermetically sealed stainless steel pans, a weighed mass of water added (30 mg for the excess water samples), and heated at a rate of 2.5°C min^{-1}. It was found that between three and four thermal cycles through the chain–melting transition were necessary to ensure that samples were homogeneous. Although this procedure made individual samples very reproducible, there was a significant variation between samples and these are the errors quoted in the text.

2.5. Density measurements

A Paar Scientific DMA 602 Digital Density meter and DMA 60 processing unit was used to determine the partial specific volumes of the fully hydrated PC/FA mixtures at 10°C below and above the chain–melting transition for each chain length. The instrument was calibrated using liquids of known density. Although the instrument itself is of high accuracy, the error in the lipid mixture partial specific volumes is estimated to be as large as ± 0.010 $\text{cm}^3\ \text{g}^{-1}$, due to difficulties in filling the U-shaped oscillator tube homogeneously with sample.

3. Results

3.1. Dry PC / FA (1:2, mol / mol) mixtures

We examined the phase behaviour of saturated PC/FA mixtures of chain lengths C_{12}, C_{14}, C_{16}, C_{18} and C_{20}. In the dry state these all exhibit sharp chain melting transitions (temperature T_m) from the untilted L_β gel phase directly to the inverted hexagonal H_{II} phase (note that our use of the word 'gel' refers to the phase structure, and does not necessarily imply the presence of water). It is interesting to note that, for these mixtures, water is not required for the formation of the lamellar gel phase. As an example, a continuous temperature X-ray scan for the dry C_{20} PC/FA 1:2 mixture is shown in Fig. 1. At low temperatures the low angle region has Bragg peaks in the ratio 1, 2, 3, 4...(6 orders are visible in Fig. 1 on the original X-ray film), characteristic of a lamellar phase, while the wide angle region has a single, quite sharp peak (full width at half maximum (FWHM) of $\Delta s = 0.004\ \text{Å}^{-1}$) at a spacing of 4.13 ± 0.01 Å at 25°C. This is characteristic of the L_β gel phase, in which the stiff and fully extended (essentially all-*trans*) hydrocarbon chains are packed in a hexagonal array, with rotational disorder about their long axis, on a timescale of 10^{-7} sec. When the temperature reaches 80°C, the low angle pattern changes abruptly to the ratio 1, $\sqrt{3}$, 2, and the wide angle peak at 4.1 Å is replaced by a diffuse peak centred at a spacing of 4.6 Å. This shows that, upon chain melting, the gel phase transforms directly to the inverse hexagonal H_{II} phase, for which the reciprocal spacings are given by $s_{hk} = d_{hk}^{-1} = 2(h^2 + k^2 + hk)^{1/2}/\sqrt{3}a$. Similar results were obtained for 1:2 PC/FA mixtures of each of the other chain lengths. The temperatures at which the diffraction patterns change agree well with

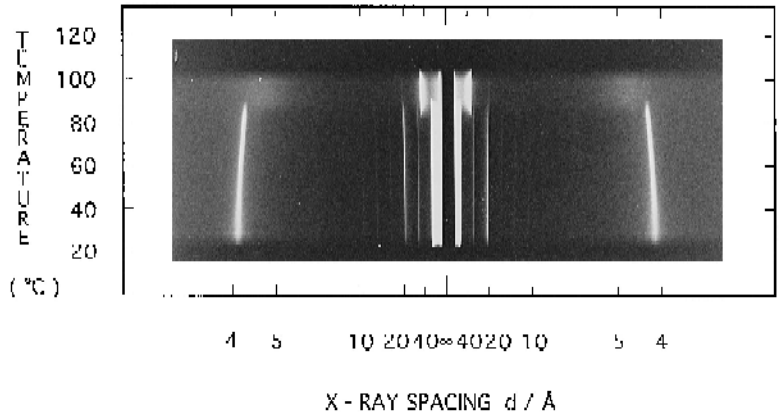

Fig. 1. A continuous temperature X-ray diffraction scan of the dry C_{20} PC/FA 1:2 mixture over the range 25–100°C. The heating rate was 20°C/h, and the film scan rate was 0.15 mm/min. The first order layer reflection of the L_β gel phase is over-exposed. For the H_{II} phase, only the 1 and $\sqrt{3}$ low angle peaks are visible.

the single, sharp calorimetric transitions observed by DSC (see, for example, the DSC scan of 1:2 DPPC/PA shown in Fig. 3).

The chain length dependence of the lattice parameters of the L_β and H_{II} phases are plotted in Fig. 2, at 10°C below and above T_m respectively. Note that, for the H_{II} phase, the lattice parameter a (cylinder centre–centre distance) is related to the lowest order d spacing by $a = (2/\sqrt{3})d_{10}$. The errors we quote for the H_{II} lattice parameter measurements were estimated from sample to sample variation, which was greater than our measurement precision. Sample to sample variation in the L_β phase was comparable to the precision of our X-ray measurements. Given that the measurements of both of these phases were made on the same samples, the explanation for the greater variation observed in the H_{II} phase is unclear.

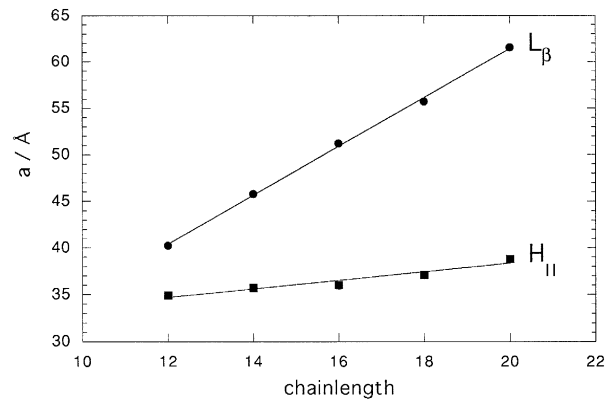

Fig. 2. The chain length dependence of the lattice parameters of the L_β (dots) and H_{II} (filled squares) phases of dry PC/FA 1:2 symmetric mixtures. The spacings were measured at 10°C below T_m and 10°C above T_m, respectively. The estimated error in the spacings is ± 0.5 Å for L_β and ± 1 Å for H_{II}.

As expected, the layer spacing in the gel phase varies linearly with chain length, with an increment of 2.63 ± 0.12 Å per methylene group (two per bilayer). Comparison with the value of 2.54 Å for the distance between alternate carbon atoms in crystalline hydrocarbon chains indicates that the hydrocarbon chains in 1:2 PC/FA mixtures are largely in the all-*trans* state and lie perpendicular to the plane of the bilayer, consistent with an untilted L_β phase. Extrapolating the layer spacing to zero chain length gives an estimate for the thickness of the polar region of 9 ± 1 Å. This is slightly smaller than the value of 10.4 Å for the estimated polar region thickness of DMPC dihydrate [38]. On the other hand, saturated fatty acids have polar regions which are only 2 Å thick [39,40], predicting a disparity in total molecular length between the FA and the PC components of approximately 8 Å. It is likely that this difference causes a modified conformation and packing for the PC headgroup in the 1:2 mixtures and that this leads to the decrease in the apparent width of the polar region. The lattice parameter of the H_{II} phase also apparently has a linear dependence on chain length, whereas one would expect roughly a square root dependence. However, the gradient of the plot is small, and so, given the errors in measuring the

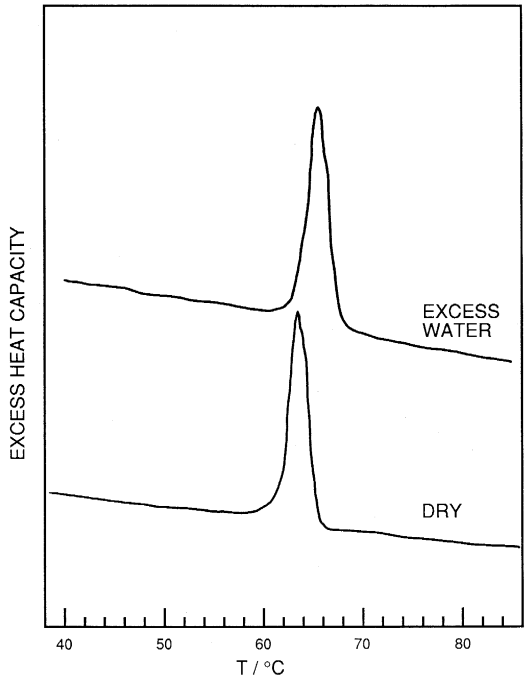

Fig. 3. DSC scans of DPPC/PA 1:2 mixtures, dry and in excess water. The heating rate was 2.5°C/min.

spacings, one should not read too much into this finding.

The d spacings of both the L_β and H_{II} phases of the dry PC/FA mixtures have been measured as a function of temperature for each chain length (data not shown). As one would expect, the temperature dependence for the L_β gel phase is small, showing a slight thinning of the bilayer due to the expansion in the lateral packing of the molecules. The temperature dependence is also quite small in the H_{II} phase. The wide-angle spacing d_{chain} from the hexagonal packing of chains in the gel phase characteristically increases to a limiting value close to 4.30 Å, reflecting the thermal lateral expansion of the hydrocarbon chain packing, just before chain melting occurs. For the L_β gel phase, the lattice parameter a_{chain} of the hexagonal chain packing is related to the wide angle d spacing by $a_{chain} = (2/\sqrt{3})d_{chain}$. The limiting value for the chain lattice parameter is thus close to $a_{chain} = 4.97$ Å, corresponding to a limiting cross-sectional area per chain of $A_{chain} = a_{chain}\ d_{chain} = 21.4$ Å^2. Assuming the chains are untilted, the interfacial area per complex, A_{comp}, is simply given by $A_{comp} = 4A_{chain}$. The value at 25°C decreases with increasing chain length, from 84.6 ± 1 Å^2 for the C_{12} mixture to 78.8 ± 1 Å^2 for the C_{20} mixture, presumably reflecting a greater van der Waal's attraction between the longer chains. From the interfacial area data at 25°C, in conjunction with the layer spacings, we calculate the molecular volume per complex to be $1{,}700 \pm 30$ Å^3 for the C_{12}, rising to $2{,}423 \pm 35$ Å^3 for the C_{20} mixture. This then gives estimates of the partial specific volumes of the 1:2 mixtures as 1.001 ± 0.017 and 0.999 ± 0.014 cm^3 g^{-1}, respectively.

3.2. Hydrated PC / FA (1:2, mol / mol) mixtures

DSC and X-ray measurements of the chain melting transitions as a function of hydration of the PC/FA 1:2 mixtures show that the gel–fluid transition temperature is remarkably insensitive to the degree of hydration. For example, Fig. 3 compares the DSC scans of a 1:2 DPPC/PA mixture in excess water with that of the dry mixture. The DSC peaks tend to broaden or even become multiple at intermediate water contents but then sharpen again in excess water (data not shown), this feature being more evident in cooling scans, and for the shorter chain length mixtures. This may be due to a tendency for the mixtures to crystallize: we, and previous workers [21,22] have observed that the gel phase of PC/FA (1:2, mol/mol) mixtures is metastable, reverting to a crystalline phase upon incubation. Another possibility is that the mixtures may tend to phase separate close to the chain melting transition. Indeed, some evidence of partial phase separation in the gel phase was observed in the X-ray patterns at intermediate levels of hydration. The small effect of hydration on the chain–melting transition of PC/FA 1:2 mixtures is in striking contrast to the behaviour of pure PC's (and indeed of nearly all other phospholipids), whose chain–melting transition temperatures progressively decrease as the hydration of the phase is increased [41]. For example, DSPC has $T_m = 98$°C in the dry state (presumably the dihydrate), which falls to $T_m = 55.5$°C when fully hydrated.

In Fig. 4 we illustrate this point by plotting T_m for PC/FA 1:2 mixtures, and for PC on its own, as a function of chain length. The hydrated and dry chain melting temperatures of the PC/FA mixtures are nearly identical, whereas the curves for the dry and fully hydrated PC's lie, respectively, above and be-

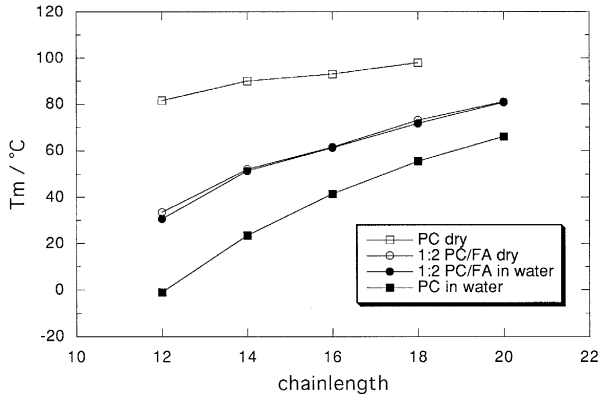

Fig. 4. The chain melting transition temperature versus chain length for dry (circles) and fully hydrated (dots) C_{12} to C_{20} PC/FA 1:2 mixtures. The data are from DSC measurements, and are estimated to be accurate to ± 1°C. Corresponding data for pure PC, both dry (open squares) (taken from [45]) and fully hydrated (filled squares) (taken from [46]) are also plotted for comparison.

low that of the PC/FA mixtures. One explanation of the hydration insensitivity of the gel–fluid transition temperature to water content might be thought to be simply that the PC/FA mixtures do not hydrate. However, our X-ray measurements (see below) clearly show that the PC/FA mixtures do, in fact, take up quite large amounts of water.

Very similar results on the transition temperatures were obtained by X-ray diffraction, although discrepancies of up to 3°C compared with the DSC values were observed. The chain-melting temperatures for the various chain length mixtures as functions of water content, as deduced by X-ray diffraction, are plotted in Fig. 5, and are essentially horizontal.

All of the PC/FA 1:2 mixtures remain in the untilted L_β gel phase upon addition of excess water. For the C_{16} and longer chain length mixtures, the chain–melting transition in excess water occurs directly to the H_{II} phase; for the shorter chain length C_{12} and C_{14} mixtures, bicontinuous cubic phases are also observed, which may coexist with the H_{II} phase [31,33,34] [1]. However, these shorter chain length mixtures form solely the H_{II} phase at lower levels of hydration.

The d spacings of the fully hydrated L_β and H_{II} phases as a function of temperature have been measured for each chain length (data not shown). The H_{II} d spacing (and hence lattice parameter $a = 2d/\sqrt{3}$) decreases with temperature, the slope becoming steeper with increasing chain length (the maximum slope is -0.2 Å/°C). The behaviour of the L_β gel phase is rather different, being essentially constant for the shorter chain lengths, yet increasing by 0.1 Å/°C for the C_{20} mixture. The wide-angle chain spacing d_{chain} increases with temperature for each chain length, reflecting a lateral expansion of the chains, to a value close to 4.3 Å at the chain–melting transition.

In Fig. 6 we have plotted the chain length dependence of the lattice parameters of the fully hydrated L_β and H_{II} phases, 10°C below and above T_m. The layer spacing of the L_β gel phase increases by 3.6 ± 0.2 Å per methylene group, which is significantly larger than the distance of 2.54 Å between alternant carbon atoms in an all-*trans* chain. Assuming the gel phase is untilted, this implies that the water layer thickness increases by approximately 1 Å per methylene group; that is, there is an increase in the limiting hydration with increasing chain length. Indeed, this is confirmed by the measured limiting hydrations re-

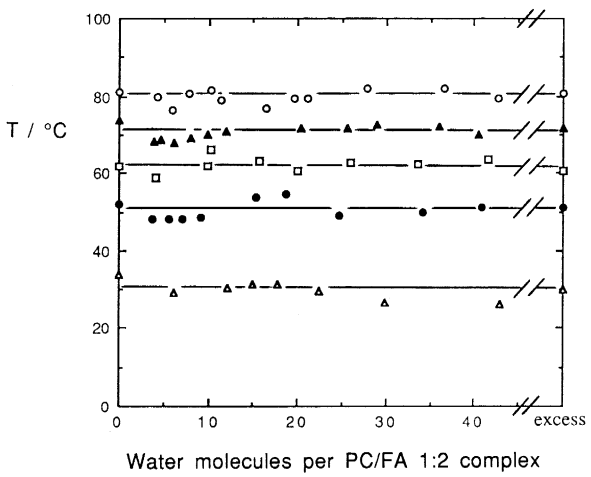

Fig. 5. The chain–melting transition temperature versus water content for C_{12} (open triangles), C_{14} (dots), C_{16} (open squares), C_{18} (filled triangles) and C_{20} (circles) PC/FA 1:2 symmetric mixtures. The data presented are from X-ray measurements, and are estimated to be accurate to ± 2°C.

[1] A separate paper will describe the complex cubic phase behaviour of C_{12} and C_{14} PC/FA mixtures (R.H. Templer, J.M. Seddon, N.A. Warrender, A. Syrykh, Z. Huang, P. Duesing, R. Winter and J. Erbes, submitted for publication).

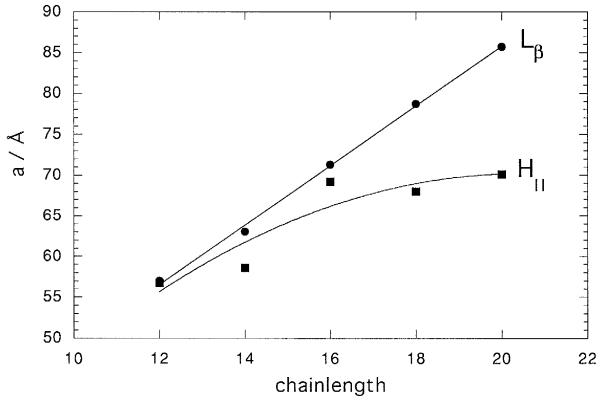

Fig. 6. The chain length dependence of the lattice parameters of the L_β (dots) and H_{II} (filled squares) phases of PC/FA 1:2 symmetric mixtures in excess water. The spacings were measured at 10°C below T_m and 10°C above T_m, respectively. The fitted line through the H_{II} data is merely to guide the eye.

ported below in Table 3. The increment per CH_2 group in the lattice parameter of the H_{II} phase is not constant but becomes progressively smaller towards longer chain lengths (the lattice parameter should roughly scale with the square root of the chain length).

As shown in Fig. 7 for DSPC/SA 1:2 mixtures at 25°C, the wide angle diffraction from the chain packing in both the dry and the fully hydrated L_β phase consists of a sharp peak (FWHM = 0.004 $Å^{-1}$) at $d_{chain} = 4.15 \pm 0.01$ Å. This implies that there is little or no change in the lateral packing, and hence also the bilayer thickness, upon hydration. Hence, we can infer that the differences between the fully hydrated and the dry layer spacings should be equal to d_w.

3.3. PC / FA 1:2 mixtures at different hydrations

We measured the lattice parameters of the PC/FA 1:2 mixtures from C_{12} to C_{20} at varying degrees of hydration. As for the dry and fully hydrated DSPC/SA 1:2 mixtures (Fig. 7), there is no detectable change in the wide-angle d spacing, d_{chain}, in the gel phase with water content for any of the different chain length PC/FA 1:2 mixtures. Fig. 8 shows the change in d spacings with water content of the L_β and H_{II} phases of the C_{18} mixture, measured at 10°C below and above T_m. The d spacings reach their limiting values at 29 and 26 waters/1:2 lipid complex for L_β and H_{II}, respectively. The d spacings versus water content for the various chain length 1:2 mixtures are given for the L_β phase in Table 1 and for the H_{II} phase in Table 2, and the limiting hydrations of the two phases are given in Table 3. The limiting hydration of the L_β phase increases progressively from 24 to 31 water molecules per 1:2 complex as the chain length increases from C_{12} to C_{20}. However, the limiting hydration of the H_{II} phase is essentially independent of chain length.

The pseudo-binary phase diagrams of the C_{12} and C_{14} 1:2 mixtures in water are complicated by the appearance of bicontinuous cubic phases, and will be reported separately. Figs. 9–11 show the pseudo-bi-

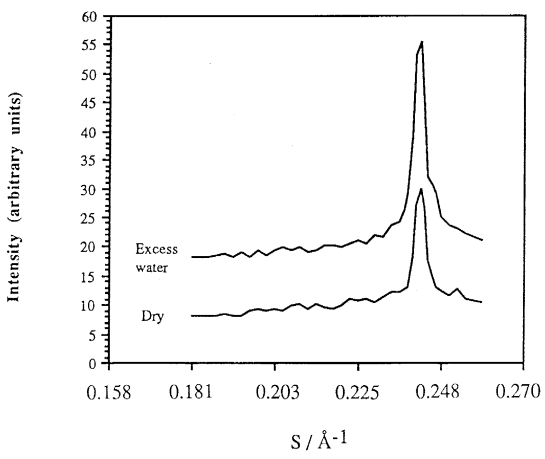

Fig. 7. The intensity profile of the wide angle diffraction peak from the L_β gel phase of dry and fully hydrated DSPC/SA 1:2 mixtures at 25°C.

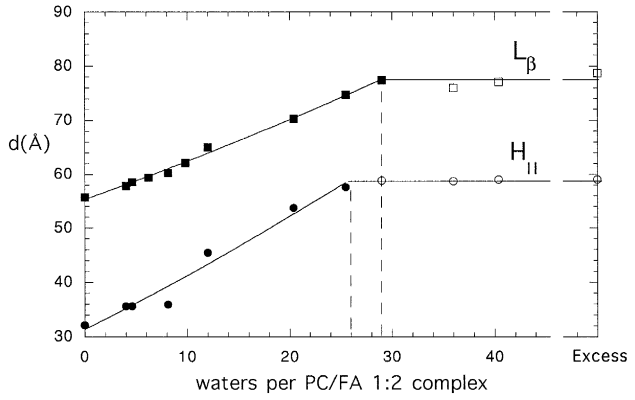

Fig. 8. The variation in the d spacings of the L_β (squares) and H_{II} (circles) phases with water content for the C_{18} PC/FA 1:2 symmetric mixtures. The fitted lines through the data are merely to guide the eye. For the composition denoted 'excess', the water content was greater than 75 wt%.

Table 1
The d spacings versus water content (moles water/mole of complex) for the L_β gel phase of the C_{12} to C_{20} PC/FA 1:2 mixtures, measured 10°C below the chain–melting transition

C12		C14		C16		C18		C20	
n_w	d (Å)	n_w	d (Å)	n_w	d (Å)	n_w	d (Å)	n_w	d (Å)
0	40.2	0	45.8	0	51.2	0	55.7	0	61.5
6.1	48.0	3.8	48.5	4.1	56.6	4.0	57.8	4.2	63.2
10.6	50.3	5.6	52.2	9.9	60.6	4.6	58.5	5.9	67.1
12.2	50.9	7.1	52.5	10.3	60.9	6.2	59.4	7.9	67.0
15.0	53.4	9.2	54.0	15.6	64.7	8.1	60.3	10.2	70.5
17.8	53.6	15.3	57.1	20.0	66.5	9.8	62.1	11.3	70.5
22.4	58.7	18.7	58.4	25.9	68.9	12.0	65.0	16.5	72.6
excess [a]	59.6	24.6	61.5	33.6	70.6	20.4	70.3	19.6	75.5
		excess [a]	62.9	41.6	69.9	25.5	74.7	21.1	77.8
				excess	71.3	29.0	77.4	27.8	81.9
						36.0	76.0	36.6	83.9
						40.4	77.1	42.7	84.9
						excess	78.7	excess	85.7

The estimated error in the spacings is ± 0.5 Å.
[a] For these chain lengths, excess denotes the limiting hydration of the L_β phase, not excess water.

Table 2
The d_{10} spacings versus water content (moles water/mole of complex) for the H_{II} phase of the C_{12} to C_{20} PC/FA 1:2 mixtures, measured 10°C above the chain–melting transition

C12		C14		C16		C18		C20	
n_w	d (Å)	n_w	d (Å)	n_w	d (Å)	n_w	d (Å)	n_w	d (Å)
0	30.2	0	30.9	0	31.2	0	32.1	0	33.6
6.1	36.6	3.8	35.5	4.1	35.6	4.0	35.6	4.2	35.2
10.6	40.3	5.6	37.8	9.9	38.3	4.6	35.6	5.9	42.3
12.2	40.7	7.1	38.6	10.3	40.1	8.1	35.9	7.9	42.5
15.0	43.7	9.2	41.2	15.6	47.9	12.0	45.4	10.2	46.4
17.8	47.1	15.3	46.1	20.0	51.7	20.4	53.7	11.3	44.8
22.4	48.7	24.6	48.2	25.9	58.8	25.5	57.6	19.6	55.3
excess [a]	50.1	excess [a]	49.9	33.6	60.8	29.0	58.8	21.1	56.0
				41.6	59.1	36.0	58.7	27.8	59.5
				excess	59.9	40.4	59.0	36.6	61.3
						excess	59.0	42.7	60.0
								excess	62.2

The estimated error in the spacings is ± 1 Å.
[a] For these chain lengths, excess denotes the limiting hydration of the H_{II} phase, not excess water.

nary phase diagrams for the C_{16}, C_{18} and C_{20} PC/FA 1:2 mixtures in water. These have very simple forms, with only the L_β gel phase and the H_{II} phase appearing at any composition, within the temperature range studied. The phase boundaries defining the limiting hydrations of each phase are close to vertical, showing that the hydration of both phases is essentially independent of temperature. Furthermore, the L_β–H_{II}

Table 3
The limiting hydrations (waters/1:2 lipid complex, mol/mol) of the L_β and H_{II} phases of C_{12} to C_{20} PC/FA 1:2 mixtures, measured 10°C below and above the chain–melting transition

Chain length	C12	C14	C16	C18	C20
L_β	24	25	28	29	31
H_{II}	24	25	26	26	24

The estimated error is ± 2 water molecules.

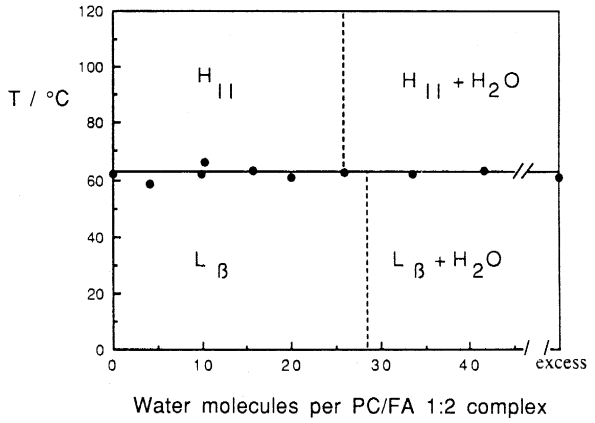

Fig. 9. The pseudo-binary phase diagram of the C_{16} PC/FA 1:2/water system. The dotted vertical lines denote that the temperature dependence of the limiting hydrations is not accurately known.

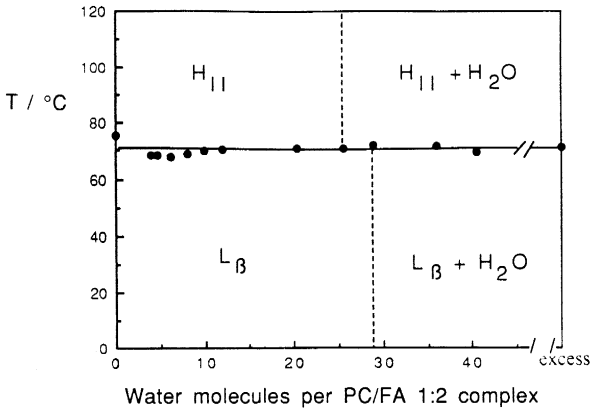

Fig. 10. The pseudo-binary phase diagram of the C_{18} PC/FA 1:2/water system.

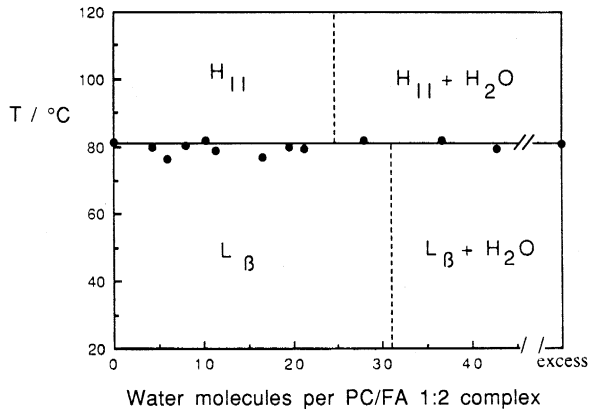

Fig. 11. The pseudo-binary phase diagram of the C_{20} PC/FA 1:2/water system.

Table 4
The partial specific volumes ($cm^3\ g^{-1}$) of PC/FA 1:2 mixtures in excess water in the L_β gel ($T_m - 10°C$) and H_{II} ($T_m + 10°C$) phases

Chain length	C12	C14	C16	C18	C20
$\bar{\nu}_{comp}$ (L_β)	0.968	0.976	0.992	0.994	1.009
$\bar{\nu}_{comp}$ (H_{II})	1.021	1.030	1.035	1.050	1.087

The estimated error is $\pm 0.010\ cm^3\ g^{-1}$.

boundaries are nearly horizontal, reflecting the fact that the chain–melting transition temperatures are nearly independent of hydration.

To allow determination of the structural parameters of the hydrated phases, we measured the partial specific volumes of these PC/FA 1:2 mixtures using an oscillating tube density meter, at 10°C below and above T_m. The results are given in Table 4. The partial specific volumes are 5–8% larger in the H_{II} phase than in the L_β phase. They increase with chain length, the gradient being 0.005 $cm^3\ g^{-1}$ per CH_2 group for the L_β phase and 0.008 $cm^3\ g^{-1}$ per CH_2 group for the H_{II} phase.

4. Discussion

4.1. Formation of PC / FA 1:2 complexes

The form of the pseudo-binary phase diagrams for FA/PC mixtures in excess water is similar to that of an azeotropic mixture [20,21], where the lower temperature phase is stabilised by attractive interactions between the components; that is, the excess Gibbs free energy is negative, making mixing more energetically favourable than the ideal case, this effect being strongest at a composition close to 1:2 (mol/mol) PC/FA. The fact that a well defined stoichiometry of 1:2 is observed for the appearance of a single sharp transition at elevated temperatures [14,20] is explained by invoking an interaction between the protonated fatty acid carboxyl group and either the non-esterified carbonyl or phosphate oxygens in the diacyl PC molecule. The fact that the effect is also observed in dialkyl PC mixtures, where the ether chain linkages are much weaker hydrogen bond acceptors, suggests that the latter possibility is more likely [27].

The gel phase of PC/FA mixtures has been reported to be metastable, reverting to crystalline bilayers upon incubation for several days at low temperatures [21,22]. These appear to be co-crystals of the stoichiometric 1:2 PC/FA mixture; that is, they probably consist of the 1:2 complex. For DPPC/PA 1:2 mixtures, the layer spacing of this crystalline phase was approximately 63 Å. We have also observed such effects for the shorter chain length PC/FA mixtures but this behaviour was not studied in any detail. For example, DMPC/MA 1:2 mixtures were found to adopt a lamellar crystalline phase with a layer spacing of 55 Å upon incubation at room temperature for 1 week (data not shown).

Interaction between the fatty acid carboxyl and the PC phosphate group would favour the mixing of the two components: indeed, our diffraction results show that phase separation of the components in the ordered phase does not occur under our experimental conditions. This appears to be in disagreement with an earlier report which claimed that, for PC/FA mixtures at neutral pH, the fatty acids are segregated into clusters within the plane of the membrane [42]. However, it should be remembered that different techniques probe different length scales: Bragg peaks in X-ray diffraction experiments arise from ordered arrays containing hundreds, if not thousands, of the basic repeat unit (individual molecules for the in-plane structure, bilayers for the lamellar ordering), and will thus not be sensitive to small-scale heterogeneities in the membrane composition. In contrast, NMR or fusion assays, which are sensitive to very local changes in composition, do give evidence of at least small-scale phase separation below the chain–melting transition [24,30]. The broadening of the DSC peaks observed under certain conditions is a further indication of partial phase separation. Furthermore, it is possible that PC/FA 1:2 complexes will form in mixtures containing low amounts of the fatty acid component but this has not been studied here and would be difficult to detect in an X-ray diffraction experiment.

A second consequence of hydrogen bonding between the fatty acid and PC headgroups might be a reduction in the hydration of the PC headgroup, since any interaction between the phosphate group and the fatty acid carboxyl would tend to reduce its ability to hydrogen bond to water. As already noted, the fatty acid component in these 1:2 PC/FA mixtures is fully protonated, even in excess water: the pK of the carboxyl group of fatty acids incorporated into PC depends somewhat on temperature and ionic strength but lies within the range 7–8.2 and this is the case over a wide range of fatty acid contents, from 0.8 to 67 mol% [24].

4.2. Chain–melting transition

As we have shown, the gel–fluid transition temperatures of PC/FA 1:2 mixtures are largely insensitive to the degree of hydration, even though it clearly remains energetically highly favourable for water to bind to the PC headgroups in these mixtures. This is a remarkable result when one considers that, for the PC component on its own, there is a large drop in T_m with hydration, of as much as 70°C for the shortest chain length studied here (C_{12}). We can understand the different behaviour of PCs and PC/FA 1:2 mixtures either by invoking thermodynamic or structural arguments. Firstly, the expected shift in the chain–melting transition temperature, T_m, from the reduction of the total free energy of the system G_m, induced by water binding to the lipid headgroups, is given [41] by: $\Delta T_m = \Delta G_{hyd,m}/\Delta S_{ref,m}$, where $\Delta S_{ref,m}$ is the transition entropy in the reference (dry) state. For pure PCs, water binds more strongly in the fluid phase, and so T_m is reduced with increasing hydration. On the other hand, for a system which can bind water equally strongly in the gel and fluid phases, ΔG_m will be the same in the reference (dry) and hydrated states and so no reduction in T_m with hydration will occur. In structural terms, we can argue as follows: Upon melting (via the pre-transition), the molecular area of PC molecules increases from a value of ca. 52 Å^2 in $L_{\beta'}$, to ca. 65 Å^2 in $P_{\beta'}$, to ca. 70 Å^2 in the L_α phase [41]. Fluidization of the lipid molecules (first the headgroups then the hydrocarbon chains) thus involves an increase in the interfacial area per molecule and, therefore, an increased accessibility of polar residues to water. Since water binding to these sites is energetically favourable, the main and pre-transition temperatures will therefore fall with increasing hydration. However, for the 1:2 PC/FA mixtures the situation is quite different. Here the PC headgroups are spaced out by the small and hydration neutral fatty acid carboxyl groups, the 1:2

complex occupying an area of ca. 85 Å^2. Thus, all the water binding sites are expected to be accessible in the gel phase and so adding water has little effect on the gel–fluid transition temperature.

4.3. Hydration and structure of the L_β gel phase

From the measured lattice parameters, the limiting hydrations of the phases and the lipid partial specific volumes, we can calculate the various structural parameters of the L_β and H_{II} phases at their limiting hydrations [43]. These structural parameters are defined in the schematic drawings of the L_β and H_{II} phases shown in Fig. 12. In the calculations, the volume fraction ϕ_{comp} of the PC/FA 1:2 complex is:

$$\phi_{comp} = \left[1 + \left(\bar{\nu}_w/\bar{\nu}_{comp}\right)(1-c)/c\right]^{-1} \quad (1)$$

where c is the total lipid weight concentration [lipid/(lipid + water)] and $\bar{\nu}_w$ and $\bar{\nu}_{comp}$ are the partial specific volumes of water and of the 1:2 lipid complex.

For the lamellar phase, the lipid layer thickness is:

$$d_l = d\phi_{comp} \quad (2)$$

and the thickness of the water layer is $d_w = d - d_l$.

The cross-sectional area per lipid complex is given by:

$$A_{comp} = 2M_r\bar{\nu}_{comp}/N_A d_l \quad (3)$$

where M_r is the molecular mass of the complex and N_A is Avogadro's number.

Since the density measurements (Table 4) were carried out in excess water, we are strictly speaking only able to calculate the structural parameters at the limiting hydration. For the fully hydrated L_β phase, the calculated structural parameters are summarised in Table 5. The values of interfacial area per complex (A_{comp}) are similar to the values of $4A_{chain}$ calculated from $A_{chain} = (2/\sqrt{3})d_{chain2}$, both at full hydration (Table 5), and as reported above for the dry mixtures in the L_β phase, when compared at the same temperature.

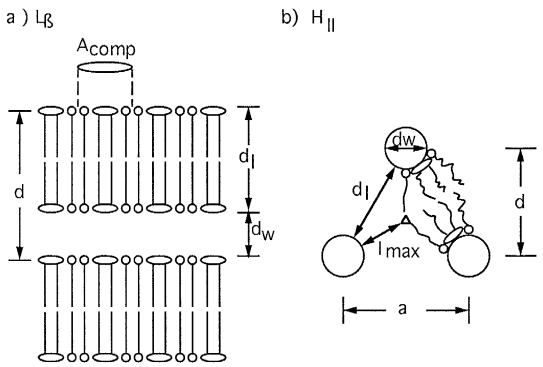

Fig. 12. Schematic drawings of the dimensions of (a) the bilayer gel phase and (b) the H_{II} phase.

Fig. 13 shows the chain length dependence of the structural parameters of the L_β phase at limiting hydration. The calculated bilayer thickness, d_l, at full hydration is essentially identical to the layer spacing of the dry 1:2 mixture for each chain length. Thus, the bilayer thickness is unchanged upon hydration. The same conclusion has been drawn from a diffraction study of DPPC oriented multilayers containing 40 mol% palmitic acid [32]. Both d_l and d_w increase linearly with chain length. The increment in d_l per methylene group is 2.6 ± 0.13 Å, consistent with an all-*trans* chain, and similar to the value observed for the dry gel phase (see above). The progressive small increase in d_w (increment per methylene group of 0.76 ± 0.13 Å) with chain length is more problematic to explain. The equilibrium distance between bilayers in lamellar phases is set by the balance between the attractive (van der Waals) and repulsive (hydration, fluctuation and electrostatic) transverse forces. For the PC/FA 1:2 mixtures in the gel phase both electrostatic and fluctuation repulsions should be negligible; the former because the layers are uncharged, and the latter because the bending elastic constant is undoubtedly very large. The quite large (18–24 Å) swelling of the gel phase with water must then be attributed predominantly to the hydration force. This swelling occurs with the lateral packing in the bilayer remaining essentially constant. Furthermore, as the interfacial composition of the bilayers is kept fixed, the magnitude of the interfacial polarity giving rise to the hydration repulsion should not vary with chain length. We therefore surmise that the observed increase in bilayer separation with chain length for PC/FA 1:2 mixtures is due either to a decrease in the van der Waals attraction between the bilayers, or to a slower decay in the hydration repulsion, as the bilayer thickness is increased. This therefore implies either that the Hamaker constant, H_A, decreases with chain length, or that the decay length, λ, for the

Table 5
The structural parameters of the L_β gel phase of PC/FA 1:2 mixtures at limiting hydration, measured 10°C below the chain–melting transition

Chain length	C12	C14	C16	C18	C20
M_r (g mol^{-1})	1022.4	1134.6	1246.8	1359.5	1471.2
ϕ_{comp}	0.696	0.709	0.708	0.717	0.723
d (Å)	58.6	62.6	70.6	77.3	84.8
d_l (Å)	40.8	44.4	50.0	55.4	61.3
d_w (Å)	17.8	18.2	20.6	21.9	23.5
A_{comp} (Å^2)	80.6	82.8	82.2	81.0	80.4
$4A_{chain}$ (Å^2)	86.5	83.1	82.4	82.3	83.4

The spacings are averaged over the data points beyond the limiting hydration, and thus differ slightly from the excess water values quoted in Table 1. The estimated error in the spacings is ± 0.5 Å, and in the areas is ± 2 Å^2.

hydration repulsion increases slightly with chain length.

Combining the facts that the chain–melting transition temperatures are essentially independent of hydration and that, in the gel phase, both the bilayer thickness d_l and the hexagonal chain packing are unchanged with varying water content, we conclude that there is essentially no effect of water on the bilayer structure in the gel phase for the PC/FA 1:2 complexes.

It is instructive to compare the maximum hydration of the gel phase of pure PC with that of the corresponding PC/FA 1:2 mixtures. For pure DSPC at limiting hydration in the tilted $L_{\beta'}$ gel phase, the water layer thickness is $d_w = 19.6$ Å and the interfacial area per molecule is 51.6 Å^2 [44]. This corresponds to 17 waters per DSPC molecule. Comparison with the value of 29 waters per DSPC/SA 1:2 complex (Table 3) shows that the gel phase of the 1:2 complex is significantly more hydrated than the corresponding gel phase of pure PC. Similarly, the DPPC $L_{\beta'}$ gel phase at 25°C has a limiting hydration of 14 waters per lipid, compared to 28 waters for the DPPC/PA 1:2 complex in the L_β gel phase (Table 3). It should be noted that, when the comparison is made *per hydrocarbon chain*, then the limiting hydrations of PC and 1:2 PC/FA mixtures are quite similar.

The formation of an untilted L_β gel phase for PC/FA 1:2 mixtures is primarily due to the fact that the fatty acids act as hydration neutral spacers between the PC headgroups, allowing them to hydrate maximally with the hydrocarbon chains remaining in their energetically preferred untilted packing. It is possible that a further factor is a reduced hydration of the headgroup region, due to residual hydrogen bonding between the fatty acid carboxyls and the phospholipid headgroup, reducing the effective hydrophilicity of the latter. However, this latter suggestion does not seem very likely, given that the gel phase of the 1:2 PC/FA complex is more hydrated than a PC gel

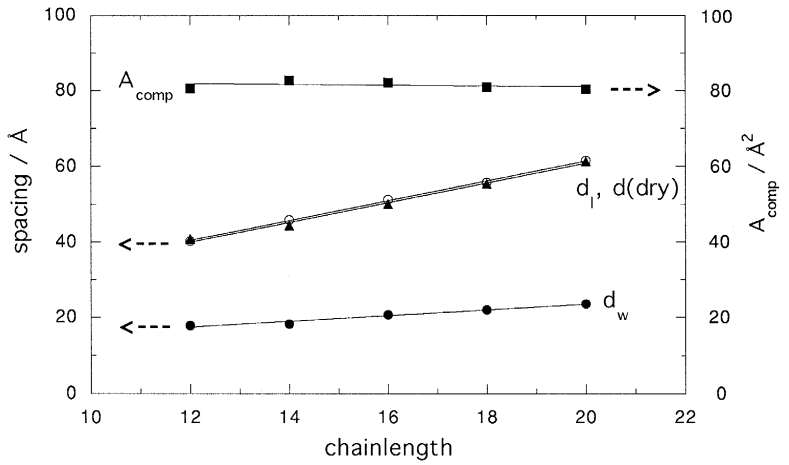

Fig. 13. Chain length dependence of the structural parameters of the L_β phase of PC/FA 1:2 symmetric mixtures at limiting hydration, at 10°C below the chain–melting transition. The quantities plotted are the lipid layer thickness d_l (filled triangles), the water layer thickness d_w (dots) and the area per complex A_{comp} (filled squares). For comparison, the d spacings of the dry mixtures (circles) are also plotted.

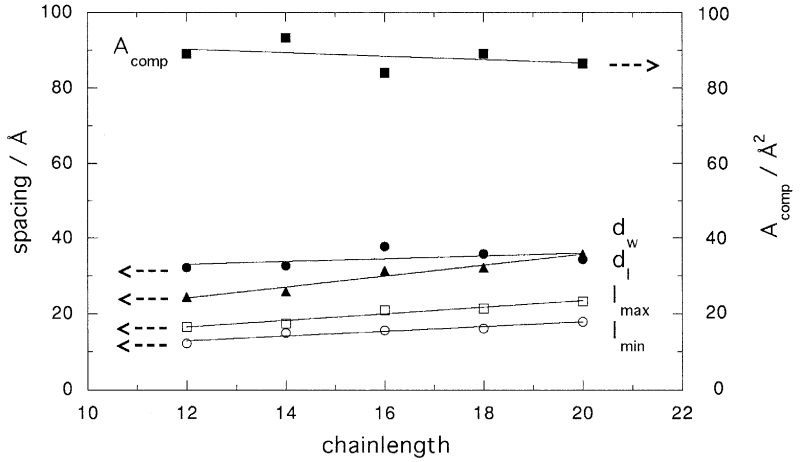

Fig. 14. Chain length dependence of the structural parameters of the H_{II} phase of PC/FA 1:2 mixtures at limiting hydration, at 10°C above the chain–melting transition. The quantities plotted are the lipid layer thickness d_l (filled triangles), the water layer thickness d_w (dots), the maximum and minimum thicknesses, l_{max} and l_{min}, of the hydrocarbon region (open squares and circles, respectively), and the area per complex A_{comp} (filled squares). The straight lines through the points are merely to guide the eye.

phase without the fatty acid present, as discussed above.

4.4. Structure of the H_{II} phase

For the H_{II} phase, the diameter of the water cylinder is given by:

$$d_w = \left[(2\sqrt{3}/\pi)(1-\phi_{comp})a^2\right]^{1/2} \quad (4)$$

where a is the lattice parameter of the hexagonal phase ($a = (2/\sqrt{3})\ d$).

The lipid layer thickness along the line connecting the cylinder axes is then:

$$d_l = a - d_w \quad (5)$$

The half thickness $d_l/2$ gives the minimum length of a lipid complex 'molecule', l_{min}, in the H_{II} phase. The distance from the interface to the centre of the hydrocarbon region represents the maximum length, l_{max}, and this is given by:

$$l_{max} = a/\sqrt{3} - d_w/2 \quad (6)$$

The area per complex at the lipid/water interface is given by:

$$A_{comp} = 2\pi d_w Mr\bar{v}_{comp}/\left(\sqrt{3}a^2\phi_{comp}N_A\right) \quad (7)$$

The chain length dependences of the structural parameters of the H_{II} phase at limiting hydration are shown in Fig. 14, and are summarised in Table 6. In the H_{II} phase at limiting hydration, the layer thickness (along the line connecting the cylinder axes) increases roughly linearly with chain length. Both l_{max} and l_{min} also increase smoothly with chain length. However, the water cylinder diameter in the H_{II} phase with chain length shows a lot of scatter, with an apparent maximum at C_{16} (see Fig. 14). Note that, on transforming from the L_β phase to the H_{II} phase, there is very little change in interfacial area per molecule at the lipid/water interface for these 1:2 PC/FA mixtures (see Tables 5 and 6).

Table 6
The structural parameters of the H_{II} phase of PC/FA 1:2 mixtures at limiting hydration, measured 10°C above the chain–melting transition

Chain length	C12	C14	C16	C18	C20
ϕ_{comp}	0.707	0.718	0.730	0.748	0.781
d_{10} (Å)	49.1	50.7	59.9	58.9	60.8
a (Å)	56.7	58.6	69.2	68.0	70.1
d_w (Å)	32.2	32.7	37.8	35.8	34.4
d_l (Å)	24.5	25.9	31.4	32.2	35.7
l_{max} (Å)	16.6	17.5	21.1	21.4	23.3
l_{min} (Å)	12.2	15.0	15.7	16.1	17.9
A_{comp} (Å^2)	89.1	93.3	84.0	89.1	86.5

The spacings are averaged over the data points beyond the limiting hydration, and thus differ slightly from the excess water values quoted in Table 2. The estimated error in the derived spacings is ±1.5 Å, and in the interfacial areas is ±5 Å^2.

4.5. Formation of the H_{II} phase

The most striking feature of 1:2 PC/FA mixtures is that they transform to non-lamellar phases directly upon chain melting, without forming a fluid bilayer phase. Although one might be tempted to suppose that a non-lamellar phase produced by addition of a single-chain amphiphile to a PC bilayer should have a type I (oil-in-water) structure, there is no doubt that the hexagonal phase of these PC/FA mixtures is, in fact, an inverted hexagonal phase of type II (water-in-oil). The fact that the phase is observed in the presence of excess water is already strong evidence for this, as a type I hexagonal phase will invariably form a micellar solution at high water contents. The crucial point is that fully protonated fatty acids are only very weakly hydrophilic and thus are almost totally insoluble in water [36]. They are essentially solubilised in the hydrated mesophase by the phosphatidylcholine component. Their effect is to alter the hydrophobic/hydrophilic balance, tending to reduce the headgroup area relative to its volume. This is mainly because two (very weakly hydrated) COOH groups will occupy considerably less area at the interface than will a strongly hydrated glycero-phosphocholine group, but may also be partly because the effective size of the PC headgroup will be reduced when it is hydrogen bonded to neighbouring fatty acid molecules (i.e., it will have a smaller hydration shell). In consequence, mesophases with lower values of interfacial area per molecule than that of the fluid bilayer (L_α) phase will be stabilised with respect to it. In other words, the gel–fluid bilayer and bilayer-inverse hexagonal transition temperatures will tend to be increased and decreased, respectively. As the latter transition is invariably of relatively low entropy, its downward shifts are expected to be larger in magnitude than the upwards shifts in the gel–fluid transition temperature. The observed findings are fully consistent with these considerations.

4.6. Implications for biomembranes

Increasingly, it has become realized that the presence in biomembranes of lipids or solutes which tend to promote non-lamellar phases may have important implications, even if non-lamellar phases themselves are not induced [47,48]. For example, the curvature stress produced in the fluid bilayer, altering the lateral stress profile across the membrane, might modulate the function of membrane proteins. Indeed, the activity of protein kinase C appears to depend on the curvature stress in the bilayer [48]. Furthermore, the presence of 'non-lamellar' lipids or solutes may promote membrane destabilization and fusion. There is now quite strong evidence that cells carefully control the spontaneous curvature of their membranes [49]. Although the present work has focused on the characterisation of the lyotropic phase stability and structure of 1:2 PC/FA mixtures, it is clear that even quite small concentrations of fatty acids in phospholipid bilayers will strongly perturb the membrane structure, at least locally, increasing the curvature stress in the bilayer, and hence potentially modulating membrane functions.

Acknowledgements

This work was supported in part by an EPSRC grant to J.M.S. (GR/C/95428), and by grants from the Deutsche Forschungsgemeinschaft to G.C. (SFB 102/D14) and to D.M. (MA 7562-2). N.A.W. acknowledges the financial assistance of the Harwell Laboratory of the UKAEA, Z.H. thanks the K.C. Wong Education Foundation and the State Education Commission of China for funding, and R.H.T. acknowledges the support of the Royal Society in the form of a Royal Society 1983 Research Fellowship.

References

[1] R. Wetzker, R. Klinger, H. Frunder, Biochim. Biophys. Acta 730 (1983) 196–200.
[2] A.M. Katz, P. Nash-Adler, J. Watras, F. Messineo, H. Takenaka, C.F. Louis, Biochim. Biophys. Acta 687 (1982) 17–26.
[3] J. Axelrod, R.M. Burch, C.L. Jelsema, Trends Neurosci. 11 (1988) 117–123.
[4] H.L. Kantor, J.H. Prestegard, Biochemistry 17 (1978) 3592–3597.
[5] C.E. Creutz, J. Cell Biol. 91 (1981) 247–256.
[6] M.J. Karnovsky, A.M. Kleinfeld, R.L. Hoover, R.D. Klausner, J. Cell Biol. 94 (1982) 1–6.
[7] L.G. Herbette, C. Fevreau, K. Segalman, C.A. Napolitano, J. Watras, J. Biol. Chem. 259 (1984) 1325–1335.
[8] R.W. Ordway, J.J. Singer, J.V. Walsh, Trends Neurosci. 14 (1991) 96–100.

[9] M.C. MacBrinn, J.S. O'Brien, J. Lipid Res. 9 (1968) 552–561.
[10] P.R. Cullis, M.J. Hope, Nature 271 (1978) 672–674.
[11] M.J. Hope, P.R. Cullis, Biochim. Biophys. Acta 640 (1981) 82–90.
[12] S. Zellmer, G. Cevc, P. Risse, Biochim. Biophys. Acta 1196 (1994) 101–113.
[13] A.W. Eliasz, D. Chapman, D.F. Ewing, Biochim. Biophys. Acta 448 (1976) 220–230.
[14] S. Mabrey, J.M. Sturtevant, Biochim. Biophys. Acta 486 (1977) 444–450.
[15] M.K. Jain, N.M. Wu, J. Membr. Biol. 34 (1977) 157–201.
[16] J.R. Usher, R.M. Epand, D. Papadjopoulos, Chem. Phys. Lipids 22 (1978) 245–253.
[17] D. Fodor, R.M. Epand, Chem. Phys. Lipids 28 (1981) 159–164.
[18] K. Lohner, Chem. Phys. Lipids 57 (1991) 341–362.
[19] D. Marsh, J.M. Seddon, Biochim. Biophys. Acta 690 (1982) 117–123.
[20] S.E. Schullery, T.A. Seder, D.A. Weinstein, D.A. Bryant, Biochemistry 20 (1981) 6818–6824.
[21] R.D. Koynova, A.I. Boyanov, B.G. Tenchov, Biochim. Biophys. Acta 903 (1987) 186–196.
[22] R.D. Koynova, B.G. Tenchov, P.J. Quinn, P. Laggner, Chem. Phys. Lipids 48 (1988) 205–214.
[23] A.B. Kohn, S.E. Schullery, Chem. Phys. Lipids 37 (1985) 143–153.
[24] G. Cevc, J.M. Seddon, R. Hartung, W. Eggert, Biochim. Biophys. Acta 940 (1988) 219–240.
[25] A.I. Boyanov, R.D. Koynova, B.G. Tenchov, Chem. Phys. Lipids 39 (1986) 155–163.
[26] J.M. Boggs, G. Rangaraj, K.M. Koshy, Chem. Phys. Lipids 40 (1986) 23–34.
[27] J.M. Boggs, Biochim. Biophys. Acta 906 (1987) 353–404.
[28] S. Zellmer, G. Cevc, J. Drug Targeting 4 (1996) 19–29.
[29] R.D. Klausner, A.M. Kleinfeld, R.L. Hoover, M.J. Karnovsky, J. Biol. Chem. 255 (1980) 1286–1295.
[30] K.P. Pauls, A.L. Mackay, M. Bloom, Biochemistry 22 (1983) 6101–6109.
[31] Y.V.S. Rama Krishna, D. Marsh, Biochim. Biophys. Acta 1024 (1990) 89–94.
[32] J. Katsaras, R.H. Stinson, Biophys. J. 57 (1990) 649–655.
[33] J.M. Seddon, J.L. Hogan, N.A. Warrender, E. Pebay-Payroula, Progr. Colloid Polym. Sci. 81 (1990) 189–197.
[34] T. Heimburg, N.J.P. Ryba, U. Würz, D. Marsh, Biochim. Biophys. Acta 1025 (1990) 77–81.
[35] V. Luzzati, R. Vargas, A. Gulik, P. Mariani, J.M. Seddon, E. Rivas, Biochemistry 31 (1992) 279–285.
[36] C. Tanford, The Hydrophobic Effect, Formation of Micelles and Biological Membranes, 2nd ed., Wiley, New York, 1980.
[37] R.H. Templer, S.M. Gruner, E.F. Eikenberry, Adv. Electron. Electron Phys. 74 (1988) 275–283.
[38] H. Hauser, I. Pascher, R.H. Pearson, S. Sundell, Biochim. Biophys. Acta 650 (1981) 21–51.
[39] V. Vand, W.M. Morley, T.R. Lomer, Acta Cryst. 4 (1951) 324–329.
[40] D.M. Small, Handbook of Lipid Research, vol. 4, Plenum Press, New York, 1986.
[41] G. Cevc, D. Marsh, Phospholipid Bilayers: Physical Principles and Models, Wiley, New York, 1987.
[42] H. Hauser, W. Guyer, K. Howell, Biochemistry 18 (1979) 3285–3291.
[43] V. Luzzati, in: D. Chapman (Ed.), Biological Membranes, vol. 1, Academic Press, London, 1968, pp. 71–123.
[44] R.P. Rand, V.A. Parsegian, Biochim. Biophys. Acta 988 (1989) 351–376.
[45] R.M. Williams, D. Chapman, Progr. Chem. Fats Other Lipids 11 (1970) 1–79.
[46] G. Cevc, Phospholipids Handbook, Marcel Dekker, New York, 1993.
[47] S.M. Gruner, Proc. Natl. Acad. Sci. USA 82 (1985) 3665–3669.
[48] R.M. Epand, Special Issue: The Properties and Biological Roles of Non-Lamellar Forming Lipids, Chem. Phys. Lipids 81 (2) (1996) .
[49] F. Osterberg, L. Rilfors, A. Wieslander, G. Lindblom, S.M. Gruner, Biochim. Biophys. Acta 1257 (1995) 18–24.